Figure S1. Distribution of collection sites for teosinte accessions used in this project. A close-up is shown for the region of origin for the Bravo accessions.
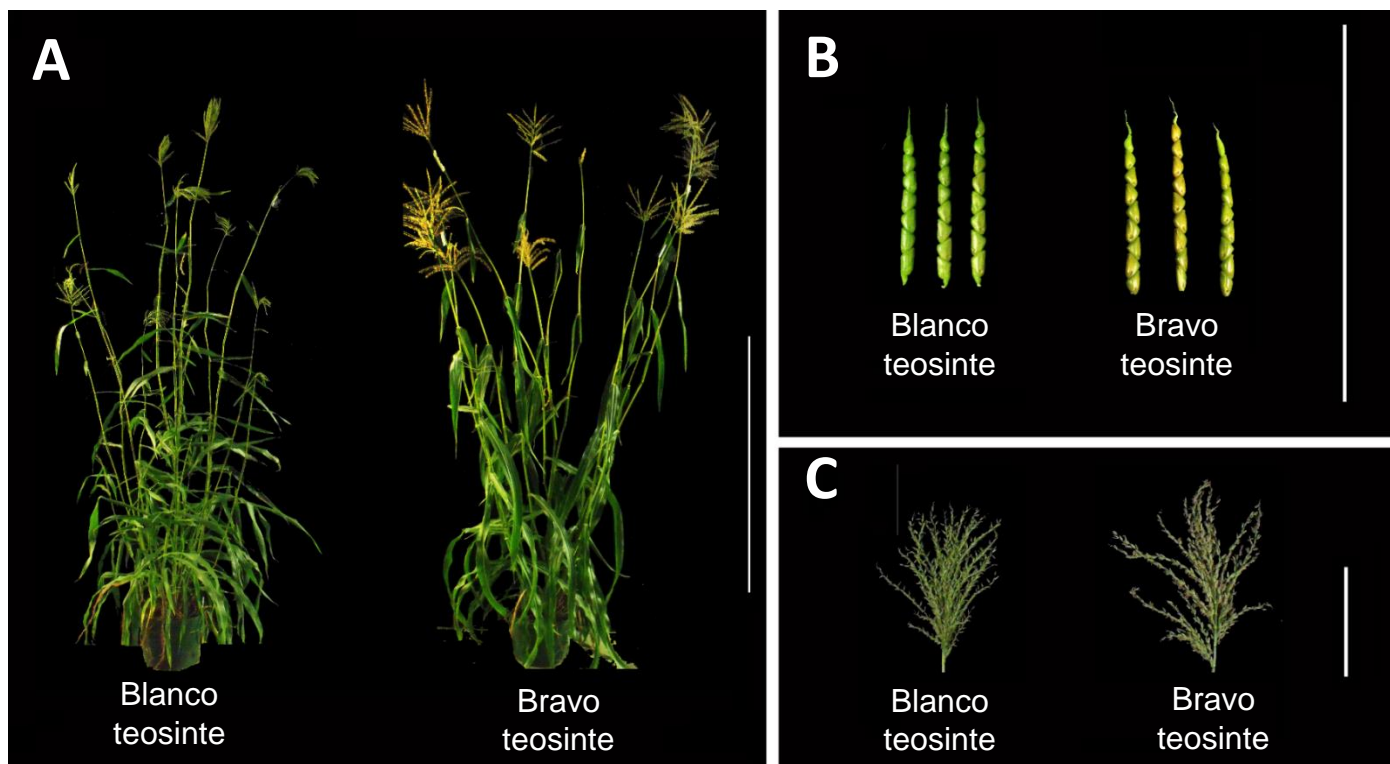
Figure S2. Teosinte plants from the Bravo and Blanco accessions. Images of whole plants (A), ears (B) and tassels (C) of Blanco and Bravo teosinte plants are shown. Scale bars represent 1 m (A), 10 cm (B, C).
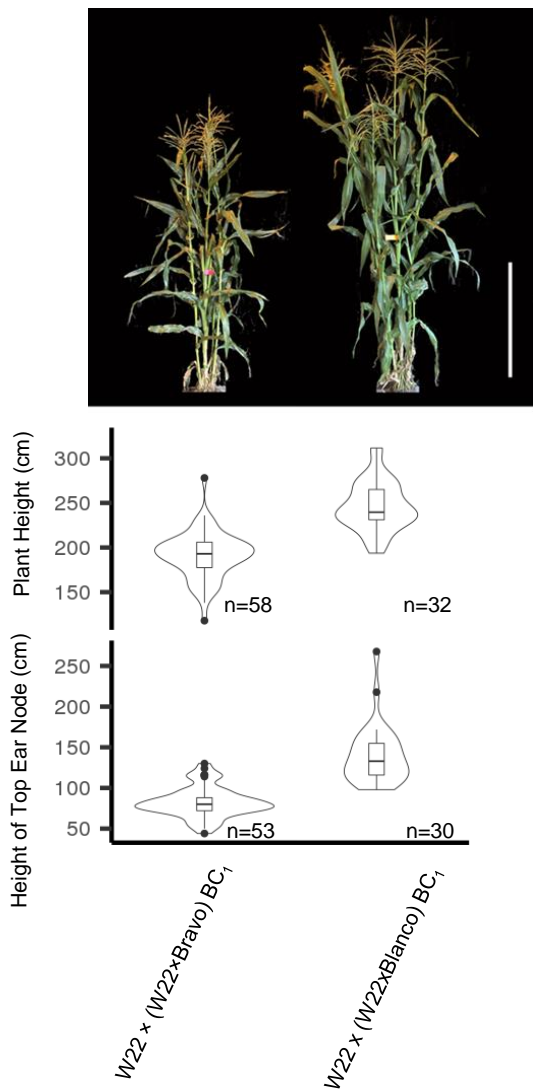
Figure S3. Phenotypic abnormalities in BC1 plants derived from crosses of the Bravo accession. A representative individuals for the BC1 of the Bravo and Blanco teosinte accessions are shown in the image. Plant height and height of the top ear node were determined for populations of BC1 plants derived from crosses of Bravo or Blanco teosinte. The number of individuals measured for each trait is indicated. Scale bars represent 1 m.
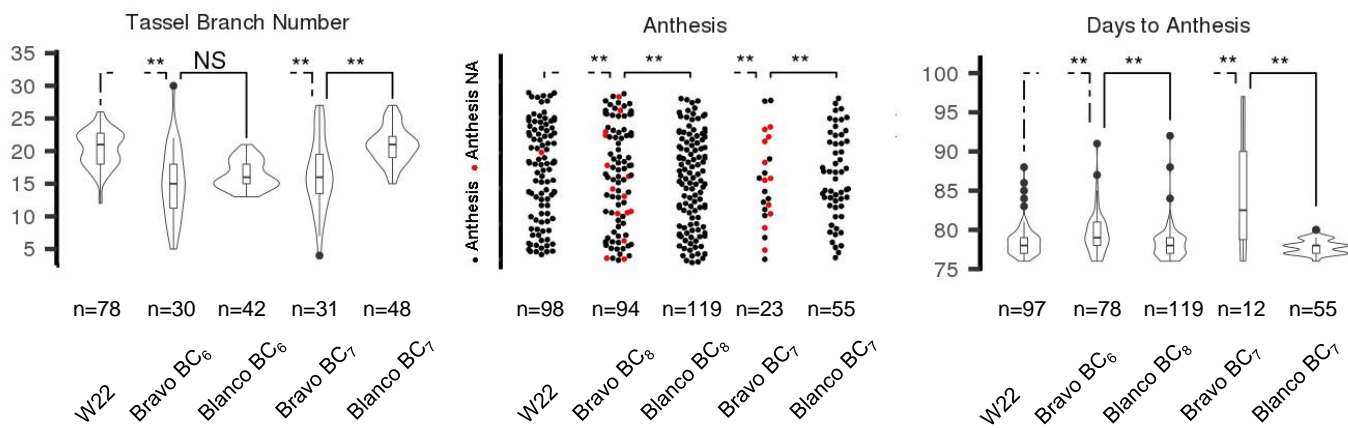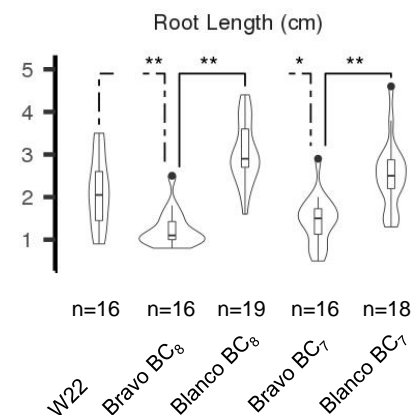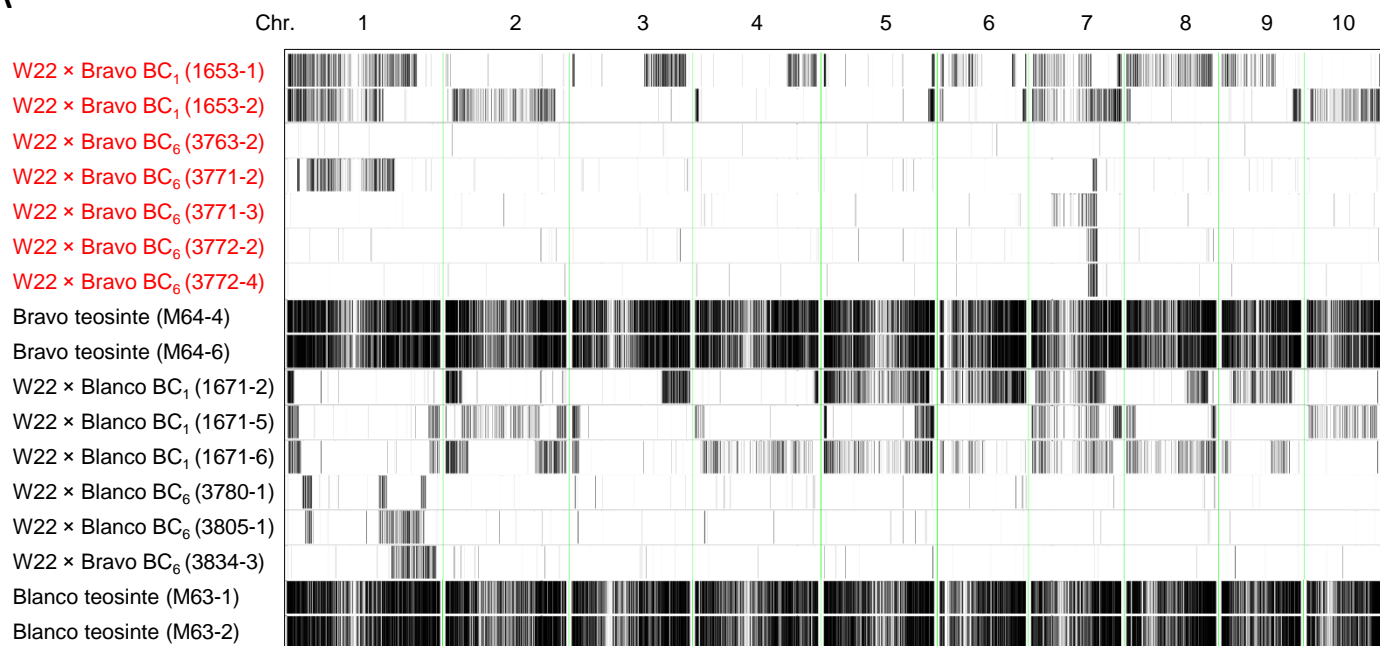
Figure S4. Phenotypic characterization of the hybrid decay syndrome. (A) Images and traits relative to male inflorescence structure and timing. (D) Seeds of W22, W22 × Bravo BC8, and W22 × Blanco BC8 were germinated for two days. The primary seedling root length was determined for each genotype. Scale bars represent 10 cm (A and B). Student's t-test was used for tassel branch number and root length, which have normal distribution. Mann-Whitney-Wilcoxon Test was used for days to anthesis and anthesis (pollen-shedding), which have non-normal distributions. *P < 0.05 and **P < 0.01. The number of plants measured for each trait (n) is listed for each plot. Two-dashed lines indicate comparisons between W22 × Bravo BC lines and W22 while solid lines indicate comparisons between W22 × Bravo BC lines and W22 × Blanco BC lines.
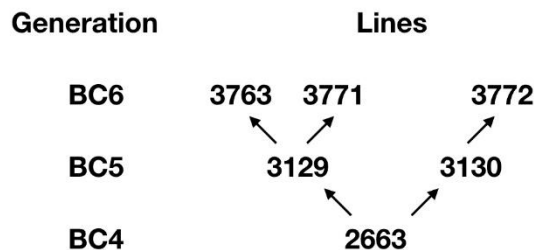
A

B

Figure S5. Documenting introgression in the backcross lines. Genotype-by-sequencing (GBS) data were generated for the teosinte accessions as well as backcross lines. The samples used for GBS analysis are shown on the left, and the red text indicates sickly plants derived from Bravo teosinte. Seed packet and plant numbers are written in the brackets. Chromosomes are drawn from left to right in order according to scale from maize B73 AGPv2 reference sequence, and the chromosome numbers are shown on the top. The vertical green lines represent the chromosome borders. The vertical black lines for each sample indicate heterozygous SNPs and the vertical black lines in the teosinte stand for the SNPs compared with W22. (B) The pedigrees (seed packet numbers) for the five W22 x Bravo BC6 plants in panel A are provided. Packets 3763 and 3771 are sibling ears derived from the same BC5. Packet 3772 represents a distinct backcross from the BC4 generation.
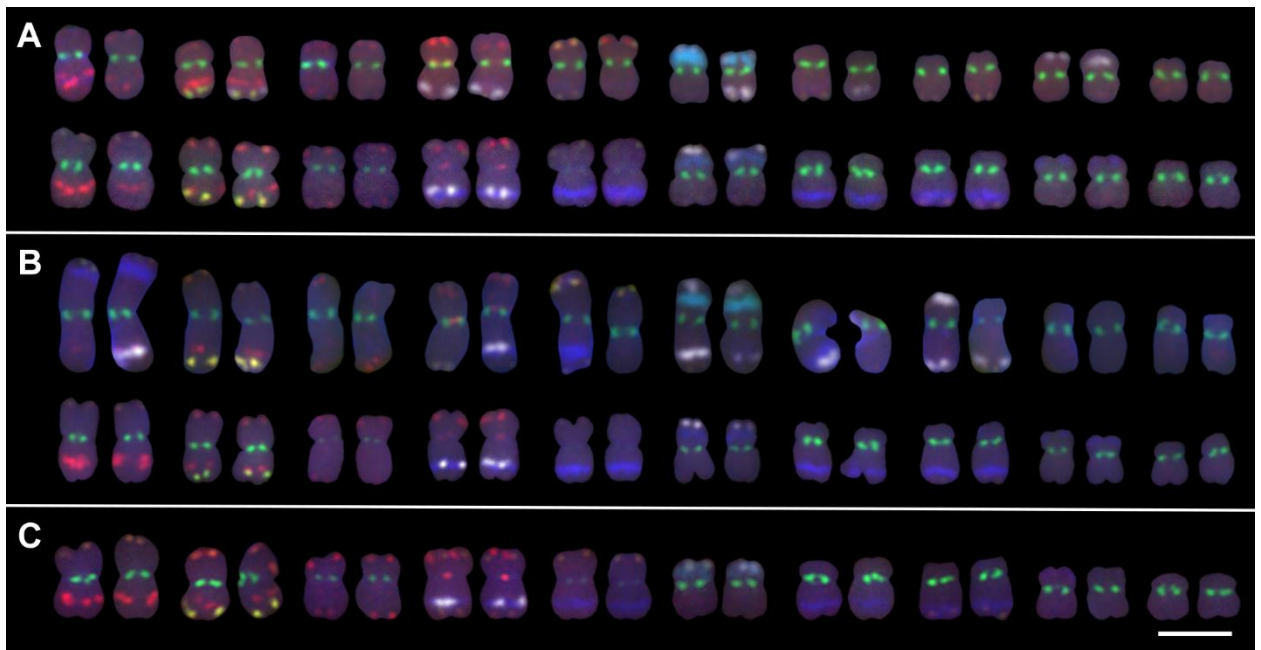
Figure S6. Karyotypes of Blanco and Bravo teosintes, W22 BC$_6$ descendants and W22 recurrent parent. (A) Top, karyotype of Blanco teosinte; bottom, W22 x Blanco BC$_6$. (B) Top, Bravo teosinte; bottom, W22 x Bravo BC$_6$. (C) W22 recurrent parent. The cytological features examined are as follows: 180-bp knob heterochromatin (blue), NOR (blue-green), CentC, subtelomere 4-12-1 (green), Cent4 (orange), TAG microsatellite, subtelomere 1-1 (red), TR-1 knob (white) and 5S ribosomal RNA (yellow). Chromosomal features are described in detail in Kato et al. (2004) and Albert et al. (2010). Scale bar, 5 μm.
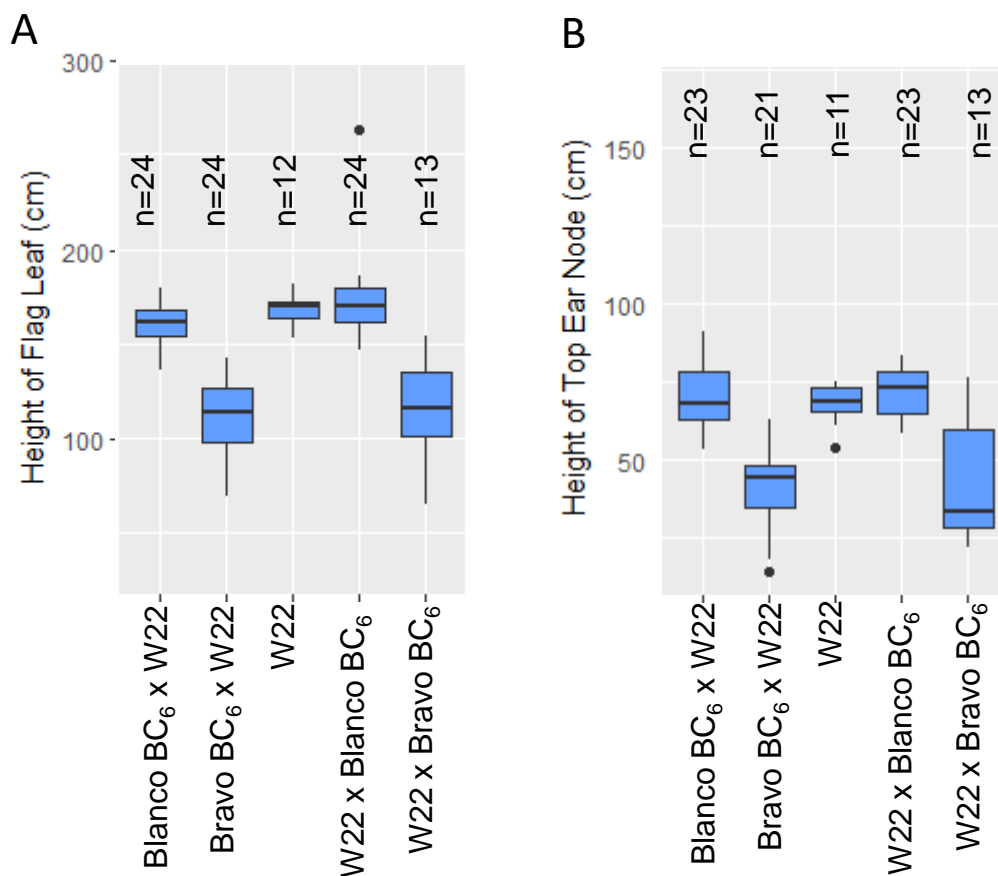
Figure S7. Transmission of hybrid decay through both male and female parents. Bravo and Blanco BC_6 plants were used to perform reciprocal crosses with W22 to generate BC_7 plants with W22 being used as either the male or female parent (the genotypes are written with the female parent listed first). The height of the flag leaf (A) or height of the top ear node (B) were measured for multiple individuals in each genotype. The sickly phenotype is observed in the Bravo BC_7 plants regardless of the direction of the cross.
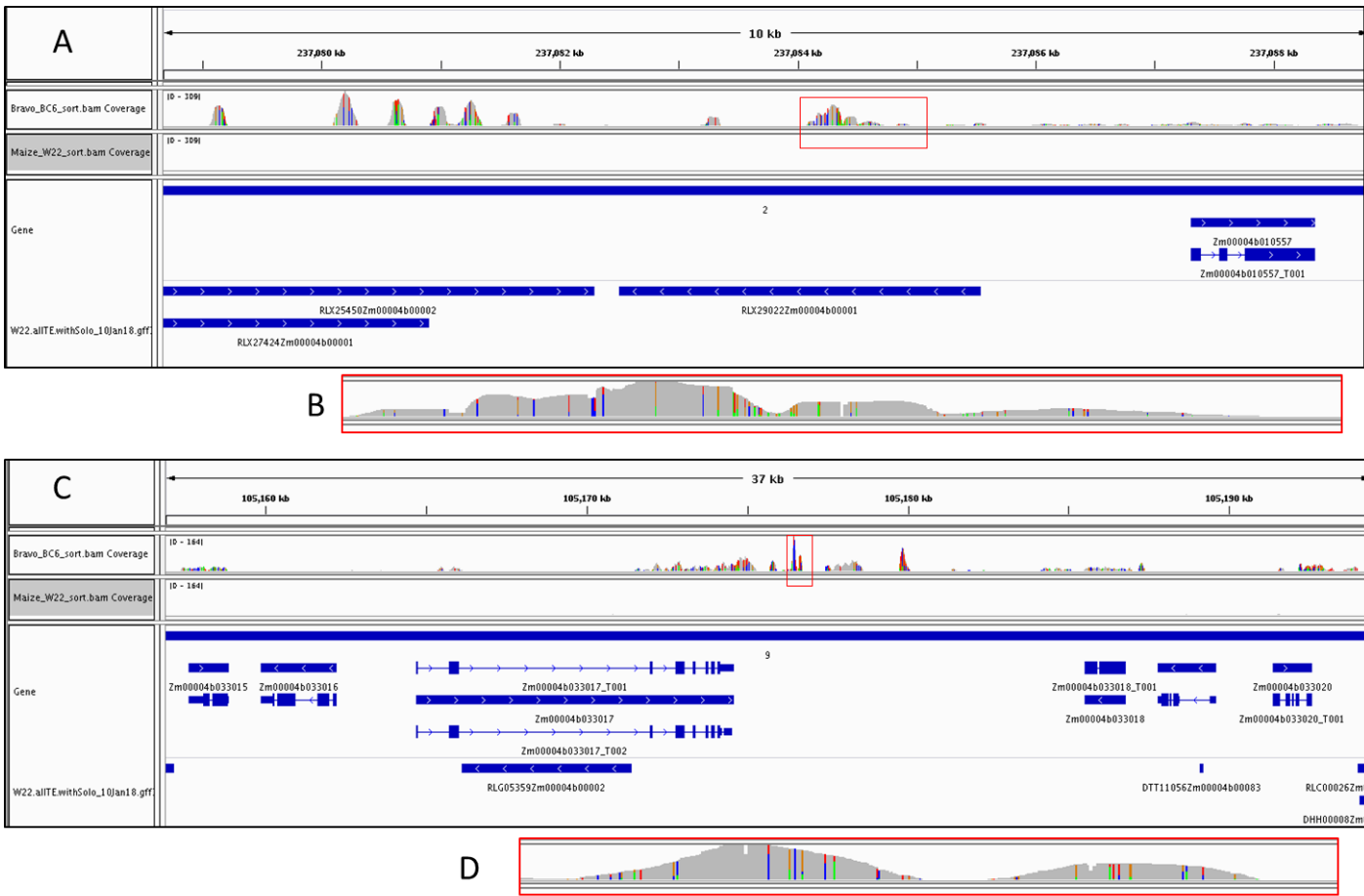
Figure S8. Examples of regions with elevated copy number when aligned to W22. Two example regions with elevated copy number in Bravo BC plants were selected for further analysis. (A,C) The WGS read depth is shown for these regions in Bravo BC_6 and W22. These visualizations also include the annotation of genes and transposable elements in the regions. The regions highlighted by red boxes indicate the regions for which coverage is shown in (B,D). In (B,D), vertical lines with color indicate the presence of a polymorphism relative to the W22 genome.
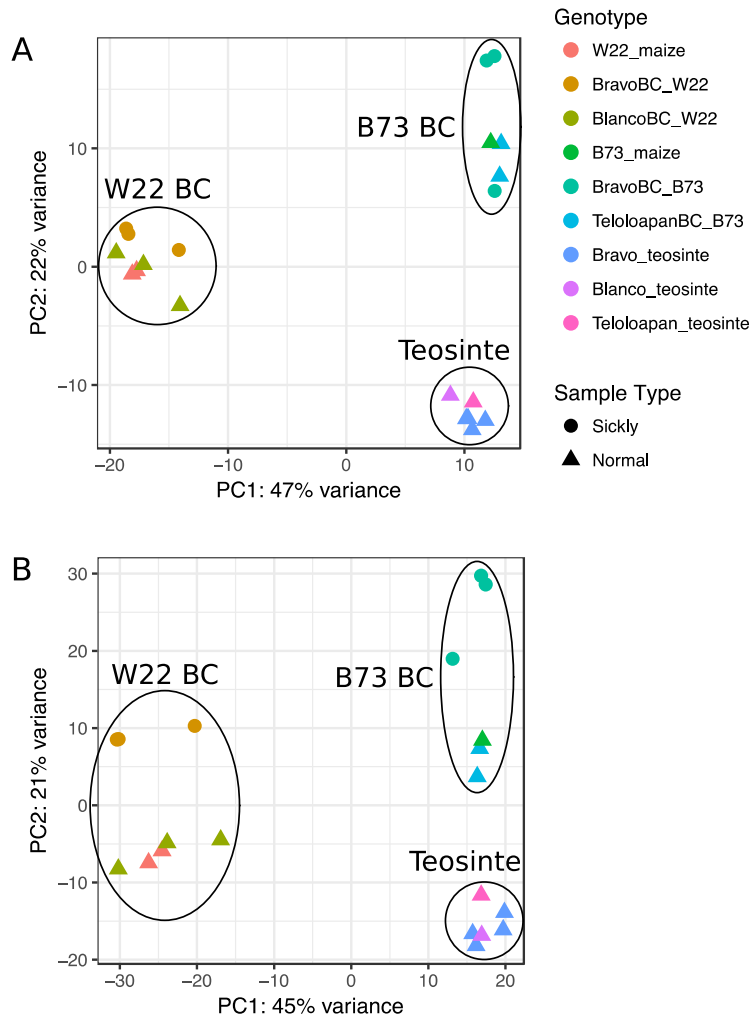
Figure S9. Principle Components Analysis based on the RNAseq data for all expressed. The PCA in (A) displays the results of PCA using the read counts for all W22 gene models after alignment of RNAseq data to the W22 reference genome. (B) A PCA was performed using the read counts from alignments of RNAseq reads to the *de novo* assembled transcripts from the W22 Bravo BC1 and BC6 individuals. The colors indicate different genotypes while the symbol shape indicates plants that exhibit the sickly syndrome (circles) and plants with normal phenotypes (triangles).
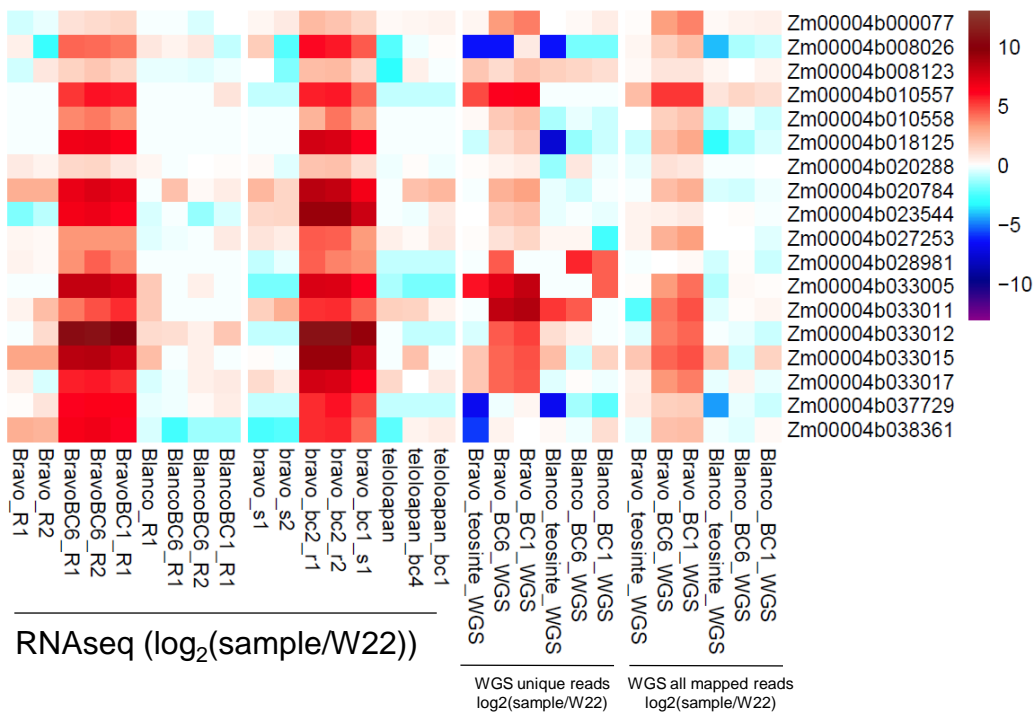
Figure S10. Changes in expression and WGS read coverage for W22 genes and transposable elements (TEs) in plants exhibiting the sickly syndrome. The alignment of RNAseq data to W22 gene models revealed 18 genes with increased expression in Bravo BC plants relative to controls. Most of these features also show increased WGS read coverage in Bravo BC plants compared to W22 when calculated using either unique-mapping or all mapped reads for genes. The color coding reflects the log2 ratio of the sample read count divided by the W22 read count with the legend on the right indicating the values.
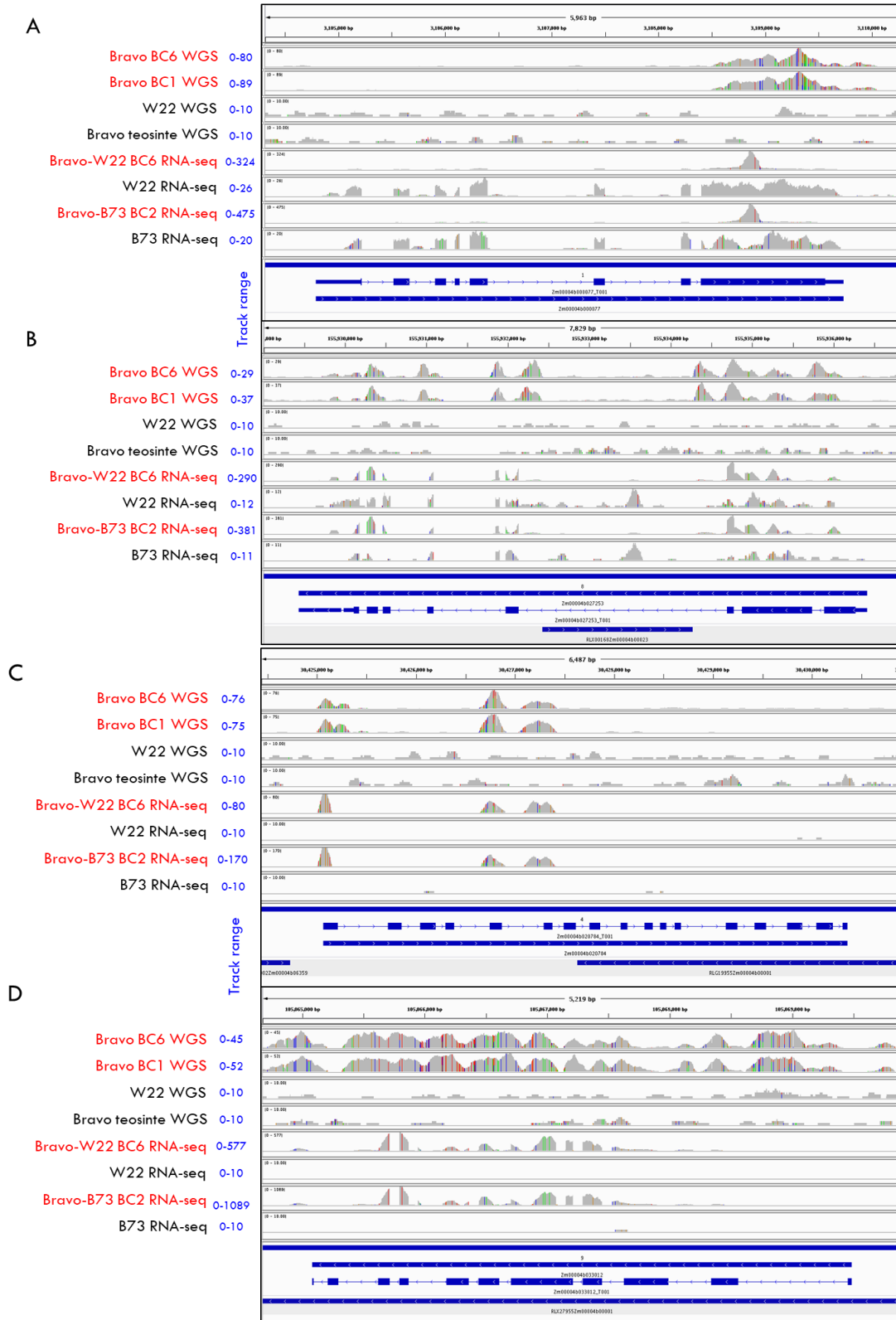
Figure S11. Examples of RNAseq and WGS coverage over genes with elevated expression. Transcribed regions of Bravo BC plants share mapping patterns and SNPs (vertical colored lines) regardless of maize genotype used in the backcross, while transcription of wild-type maize alleles show differing patterns. Transcribed regions can match high coverage regions (top) or show splicing patterns consistent with gene expression (bottom).
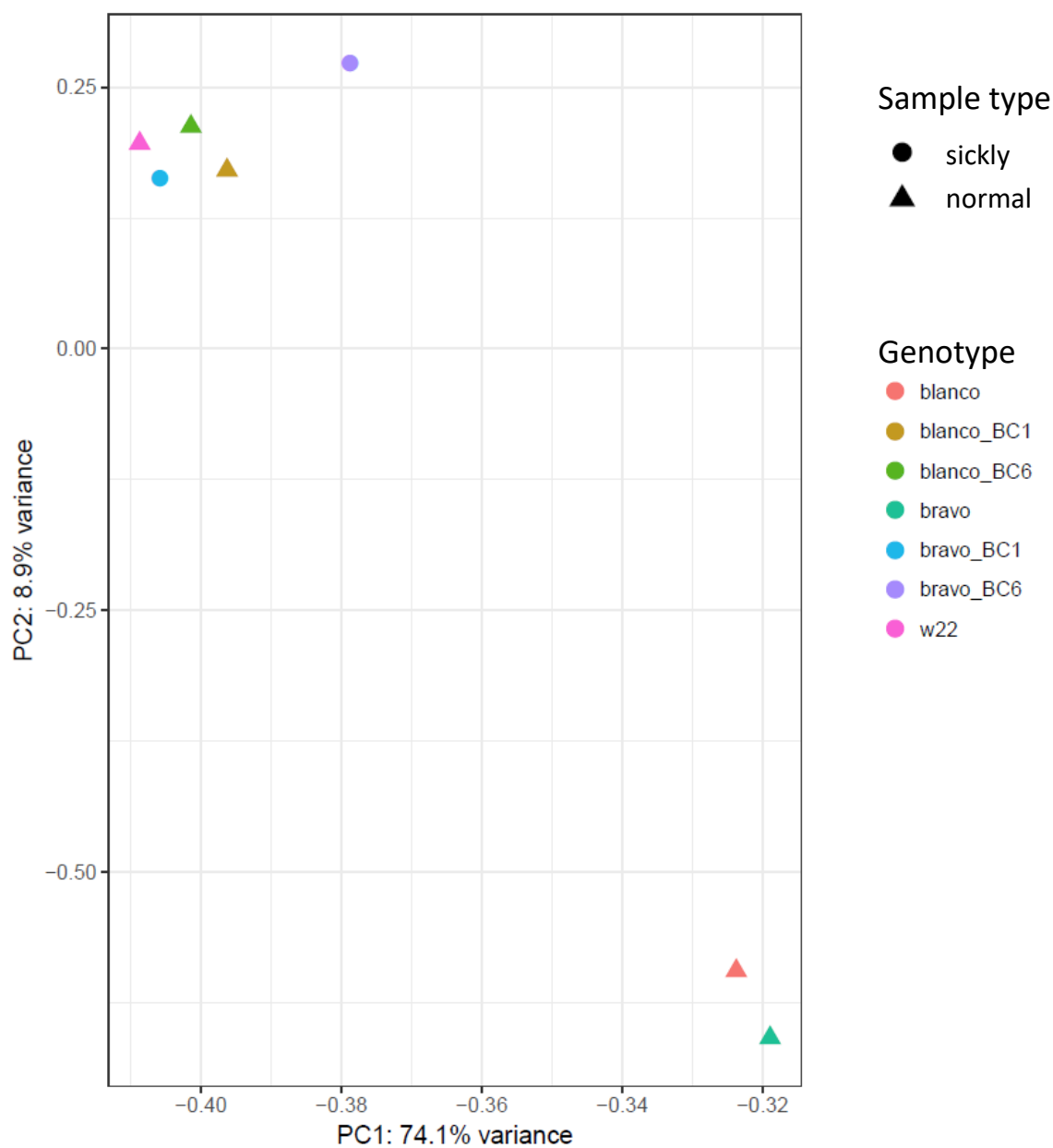
Figure S12. A principal component analysis was performed using the whole genome bisulfite sequencing data. The methylation levels for each 100bp window throughout the genome were used to perform PCA. The sample colors indicate genotypes and the symbols indicate whether the individuals exhibit the sickly phenotype (circles) or normal phenotype (triangles).
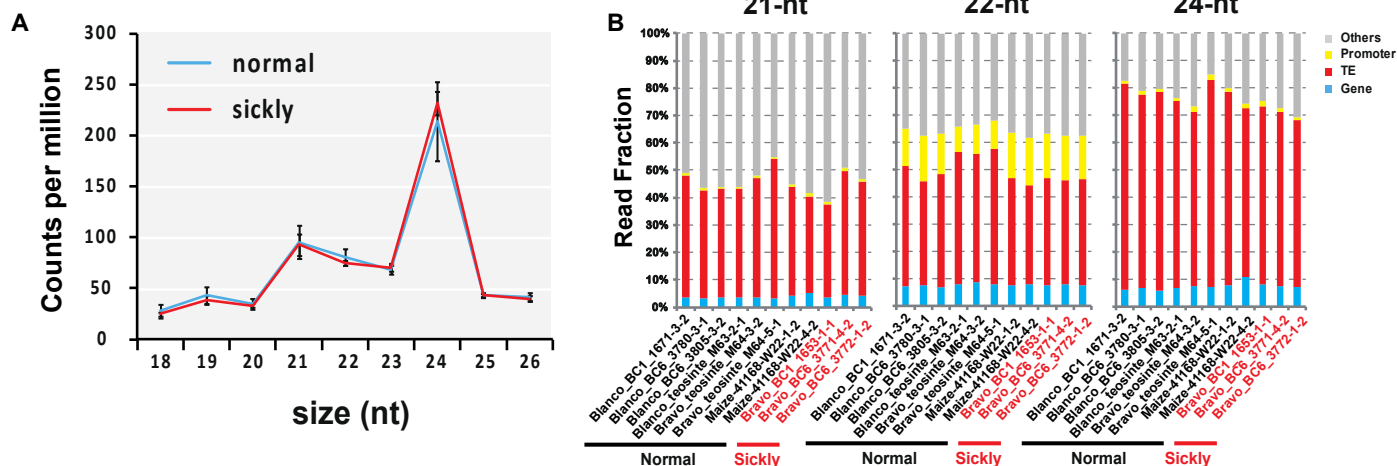
Figure S13. (A) Size (in nucleotides) distribution of sRNA in normal and sickly plants of W22 genetic backgrounds. Error bars indicate standard deviations from eight normal plants and three sickly plants with W22 genetic backgrounds. (B) Proportions of sRNA in three size classes in sickly and normal control plants.
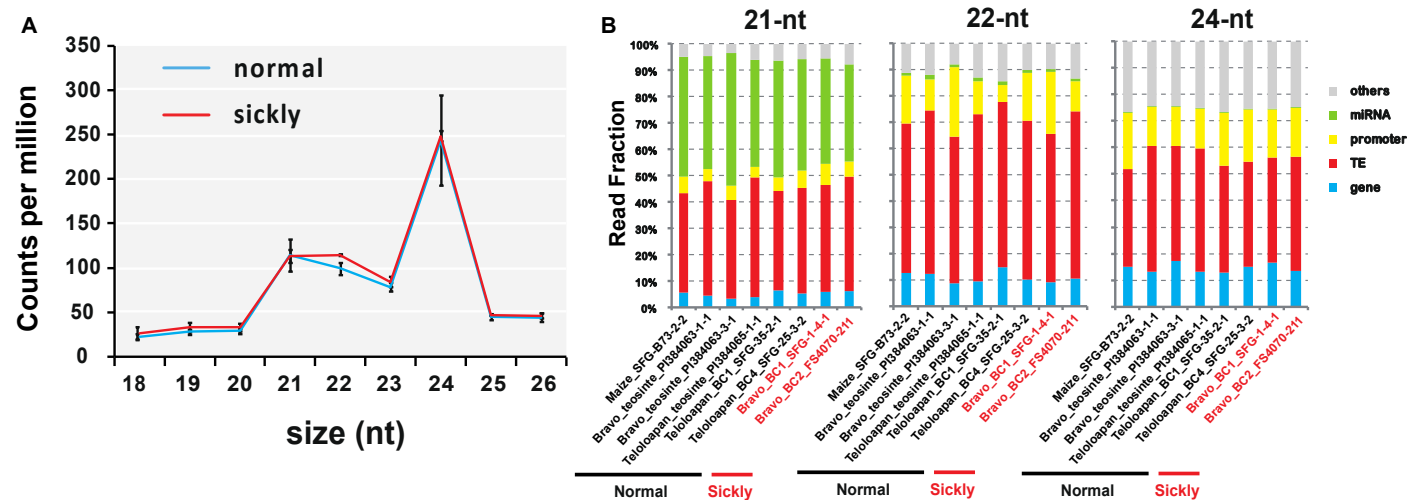
Figure S14. (A) Size (in nucleotides) distribution of sRNA in normal and sickly plants of B73 genetic backgrounds. Error bars indicate standard deviations from six normal plants and two sickly plants with B73 genetic backgrounds. (B) Proportions of sRNA in three size classes in sickly and normal control plants.
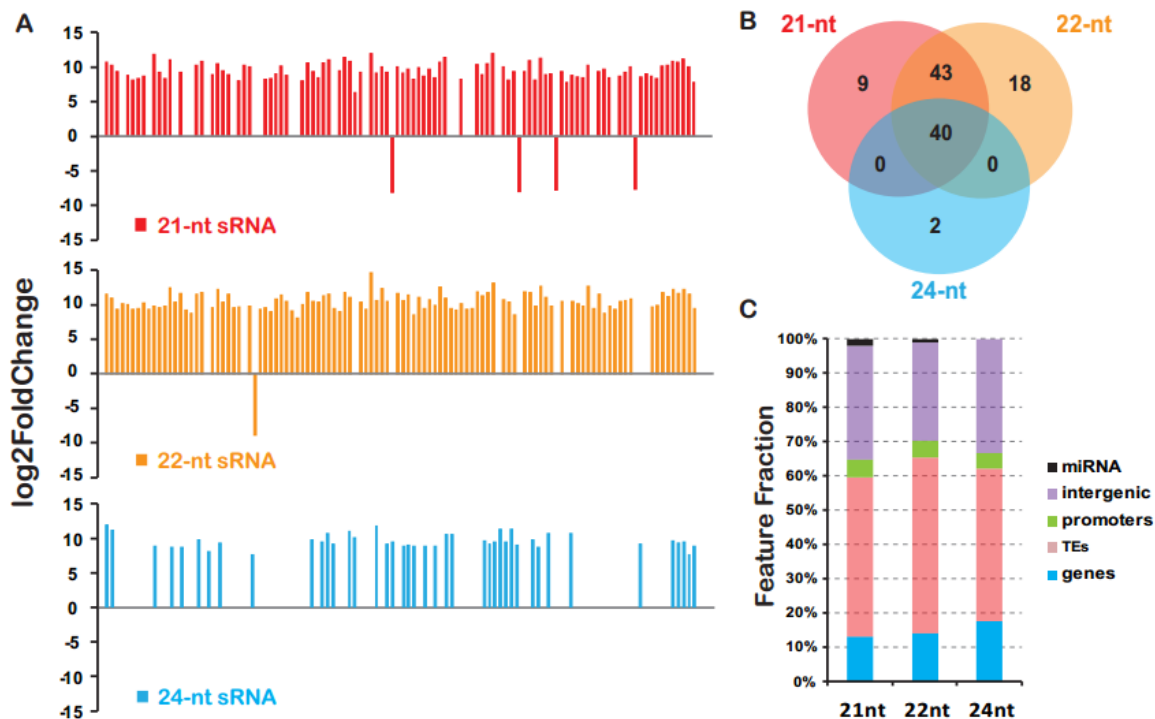
Figure S15. Feature analyses of differentially expressed sRNA regions between the sickly Bravo BC plants and the normal plants of B73 background. (A) Distribution of differentially expressed sRNA regions one-by-one that display a strong directional bias. Almost all of these differentially expressed sRNA regions produced increased 21-nt, 22-nt, and 24-nt sRNA in sickly plants compared to normal plants. The y-axis indicates the log2 transformation of fold changes, with positive value representing that increased sRNA were generated in sickly Bravo BC plants compared to the normal plants of B73 background. (B) Almost half of differentially expressed sRNA regions with increased sRNA in sickly plants produced three classes (21-nt, 22-nt, and 24-nt) of sRNAs concurrently. (C) Overlap profiling of differentially expressed sRNA regions with B73 genomic features, including genes, transposable elements (TEs), 2-kb promoter regions of annotated genes, and intergenic regions. The log2 fold change >0 means that increased sRNA were generated in sickly Bravo BC plants compared with the normal plants of B73 background. The log2 fold change <0 means that reduced sRNA were produced in sickly Bravo BC plants compared with the normal plants of B73 background.
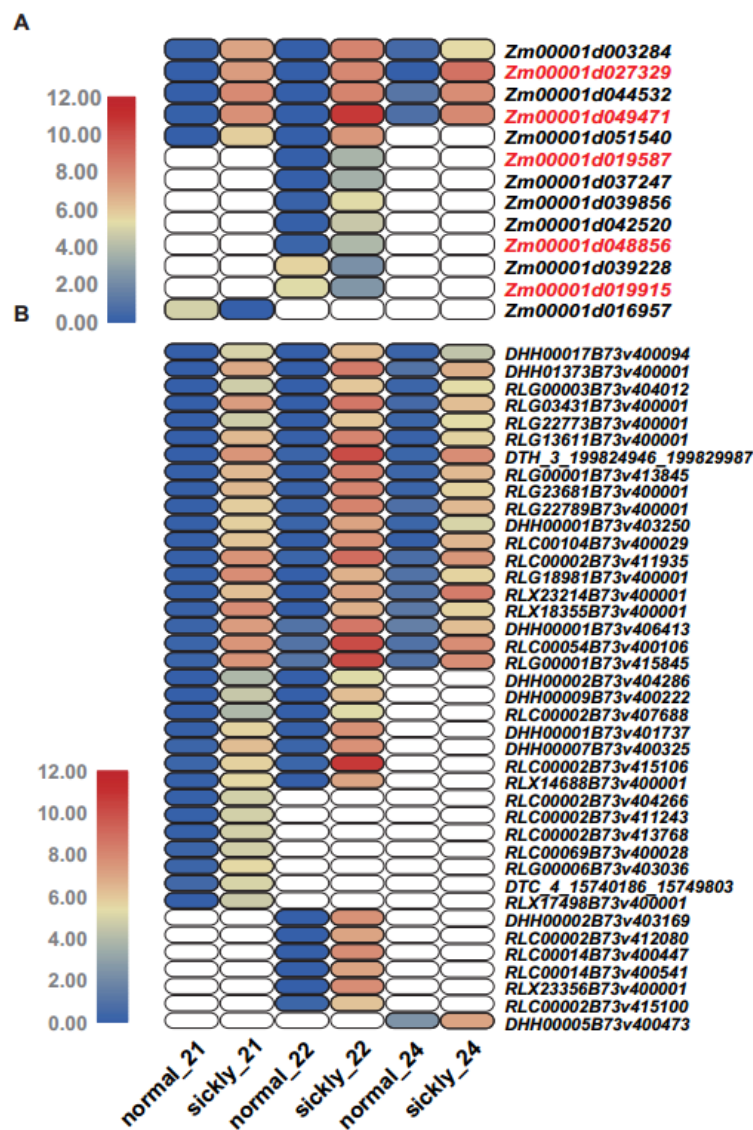
Figure S16. Annotated B73 genes (A) and transposable elements (TEs) (B) that potentially generated significantly different amount of sRNAs between normal and sickly plants and their comparisons with other features of genes or novel transcripts expression, CG or CHG DNA methylation, and WGS copy number. Genes with red fonts in upper panel indicate that the corresponding W22 homolog genes also produced more sRNA in sickly plants with W22 genetic background (see Figure 8).